Title
CORC ® cable terminations with integrated Hall arrays for quench detection

Journal
Superconductor Science and Technology, 33(9)

ISSN
0953-2048

Authors
Teyber, Reed
Marchevsky, Maxim
Prestemon, Soren
et al.

Publication Date
2020-09-01

DOI
10.1088/1361-6668/ab9ef3

Peer reviewed

CORC® Cable Terminations with Integrated Hall Arrays for Quench Detection

Reed Teyber[1], Maxim Marchevsky[1], Soren Prestemon[1], Jeremy Weiss[2] and Danko van der Laan[2]

[1]Lawrence Berkeley National Laboratory, Berkeley, CA 94720
[2]Advanced Conductor Technologies LLC, Boulder, CO 80301 and University of Colorado, Boulder, CO 80309

E-mail: rteyber@lbl.gov

Abstract.

ReBCO superconducting cables have the potential to enable compact thermonuclear fusion reactors that operate at magnetic fields exceeding 20 T and allow operation at temperatures far exceeding the boiling point of liquid helium, potentially allowing for demountable magnets. Normal zone detection remains a challenge, and while novel quench detection techniques are an active area of research, few are non-invasive, provide real-time quench detection, and have been demonstrated with current ramp rates relevant for fusion reactors. To address this problem, a CORC® cable termination is developed with integrated Hall sensors to monitor current redistribution as a proxy for quench detection. The methodology exploits the current sharing and layered topology in CORC® cables, and allows quench detection using a localized sensor instead of co-wound voltage wires or optical fibers. Experiments are presented where current redistribution is measured from induced quenches, and in a 0.2 meter CORC® sample it is found that the Hall sensors detect normal zone transitions with a similar magnitude and temporal resolution as voltage measurements. To emulate the conditions of dynamic poloidal and central solenoidal fields, experiments are repeated with ramp rates up to 10 kA/s that demonstrate the potential to detect normal zone development over a range of experimental parameters.

Keywords: High temperature superconductor, ReBCO, CORC®, CICC, quench, Hall sensor, Tokamak

1. Introduction

Rare-earth Barium Copper Oxide (ReBCO) superconducting tapes have demonstrated critical current densities exceeding 1 kA/mm^2 in 30 Tesla background fields [1], galvanizing research efforts in high-field accelerator magnets [2, 3] and compact thermonuclear fusion devices [4, 5, 6, 7]. While ReBCO superconducting cables can play an important role in providing clean and renewable electricity from fusion reactors, two challenges facing large-scale ReBCO adoption are capital cost and quench protection. Although ongoing ReBCO

procurements are expected to continuously drive costs down, additional methods are required to detect the normal zone transitions that have damaged many ReBCO coils to date.

The intrinsic thermophysical properties of ReBCO make the conductor resilient to small thermal disturbances. If a heat source is sufficiently powerful to locally transition the conductor, these properties are no longer advantageous and catastrophic levels of energy can be dissipated before the slow-moving quench wave is detected with traditional techniques. Numerous methods have been explored to supplement voltage measurements in detecting normal zone transitions, including optical fibers [8, 9], acoustic emission monitoring [10, 11], stray capacitance monitoring [12], diffuse ultrasound thermometry [13, 14, 15], quench antennas [16, 17, 18] and Hall sensors [19], to name a few. Promising results have been reported, although few are non-invasive and provide real-time quench protection. Furthermore, many of these techniques have not been demonstrated with the fast current ramp rates found in thermonuclear fusion applications [20].

Conductor On Round Core (CORC®) cables and wires from Advanced Conductor Technologies LLC (ACT) have received significant attention as flexible, high-current and low-inductance conductors for particle accelerators and fusion reactors [21, 22, 23]. Most recently, Weiss *et al* (2020) [24] presented a record CORC® engineering current density of 678 A/mm^2 at 12 T, 4.2 K and a 63 mm bend radius, which extrapolates to over 450 A/mm^2 at 20 T. To inject and extract current, CORC® cable terminations are constructed by exposing tapes from each layer along the length of a terminal [25, 26] (Fig. 1). As illustrated in Fig. 2, outer tape layers terminate close to the end of the terminal where the cable enters, and inner tape layers terminate near the opposite end of the terminal. The current sharing in this unique cable topology can be exploited to sense hot spot formation; redistribution of current in the cable manifests as an axial shift of current in the termination (solid and dotted lines in Fig. 2).

Figure 1. Photo of CORC® wire exposed into glass terminal.

Terminal Hall sensors were used to investigate joints and current dynamics in ITER central solenoid cables [27], and Marchevsky *et al* (2010) [19] measured current redistribution with Hall sensors as a method to detect quenches. In a similar methodology to Refs. [19, 27], Hall sensors can be integrated in CORC® terminals to monitor inter-tape current redistribution in cables with poor current sharing. The proposed methodology utilizes low-cost sensors and can be implemented with equipment external to the magnet.

In this work, we describe the development of CORC® wire terminations with integrated Hall arrays, and report on the ability to detect current redistribution at the onset of a quench with static and fast-ramped conditions. A campaign of tests are performed in liquid nitrogen

to characterize the magnetic field response along CORC® terminals associated with current redistribution after inducing a quench with both a heater and permanent magnet. Quench experiments are performed with current ramp rates up to 10 kA/s to emulate the conditions found in the central solenoidal coils of Tokamak reactors [20]. Insights on current sharing and redistribution in CORC® cables are explored, and the efficacy of the proposed method as a real-time quench detection method in Fusion reactors is discussed.

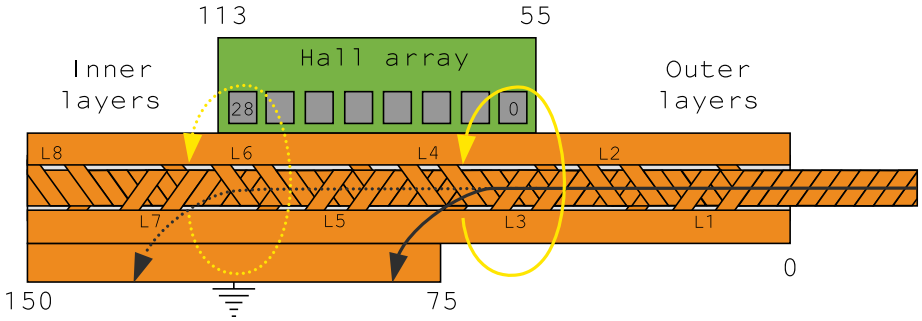

Figure 2. Illustrative schematic of CORC® terminal and Hall array. Black solid and black dashed lines show current redistributing from outer layers to inner layers, resulting in axial shift of magnetic field (yellow dotted line). Sensor 0 corresponds to the inside (right) of the terminal, and sensor 28 corresponds to the outside (left) of the terminal. Terminal block dimensions are shown in units of mm.

2. Methods

The experimental apparatus is shown in Fig. 3, consisting of a 0.2 meter long CORC® wire, two copper terminal blocks, a Printed Circuit Board (PCB) Hall sensor array containing 29 sensors, a resistive heater and a permanent magnet. In the terminations, trimmed tape layers are exposed into a 150 mm long, 6.35 mm diameter copper tube (Fig. 1) that is filled with molten indium. The cylindrical CORC® terminal is wrapped in indium foil and clamped between two copper plates (25.4 mm wide, 150 mm long and 6.35 mm thick). The assembly is fixed to a bottom copper plate (75 mm long, 6.35 mm thick) that interacts with the outermost 75 mm of the terminal. The Hall array positioning exploits the resulting current redistribution illustrated in Fig. 2.

2.1. Static quench experiments

The first set of experiments investigate the current redistribution from an induced quench with static current at 77 K. A Sorensen SGA 10/1200 power supply is ramped to a desired current, at which point a 20 W resistive heater is fired. The heater causes a normal zone transition in the outer layer that spreads both longitudinally along the conductor and radially to inner layers in the CORC® conductor. To explore the Hall sensors as a technique for quench detection, the relative changes in Hall sensor voltage are presented during this

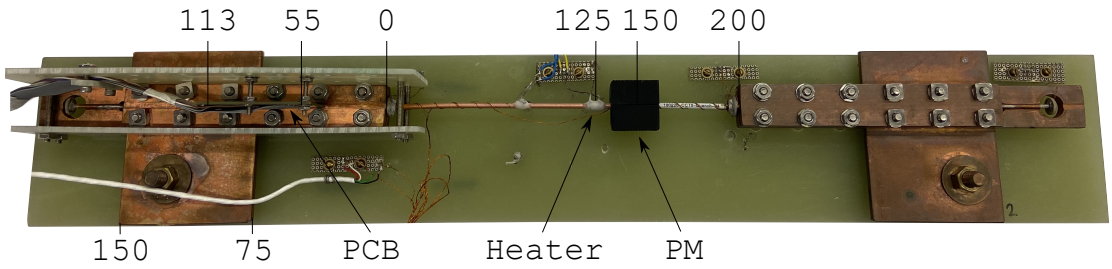

Figure 3. Experimental apparatus showing CORC® wire, terminal blocks, PCB Hall array, quench heater and Permanent Magnet (PM) fixture. Dimensions are shown in units of mm.

normal zone initiation. This is achieved by averaging each Hall sensor voltage for 5 s before inducing a quench, and subtracting it from the redistribution measurements. This facilitates visualization of magnetic field changes, and can readily be adopted for real time detection.

2.2. Dynamic quench experiments

The next set of experiments explore quenches at 77 K with ramp rates relevant for certain fusion applications. Due to varying tape inductances [9, 28], the voltage distribution in the terminal is a function of both the net current and current ramp rate. The measured current profiles used in this manuscript are shown in Fig. 4, with ramp rates of 250, 1,000, 5,000 and 10,000 A/s. All of the current ramps are from 0 to 1,000 A, where a small resistive voltage rise is observed in the CORC® conductor. To better compare the ramp profiles in Fig. 4, the x axis has been normalized over the programmed ramp duration (4, 1, 0.2 and 0.1 s, respectively). As shown in the inset, the 250 A/s ramp rate has a nonlinear profile characterized by fast, small increases in current followed by a dwell period. In contrast, the faster ramp rates follow a more linear path.

Two means of inducing a quench are employed: (1) with the aforementioned resistive heater, and (2) with a permanent magnet fixed to the conductor. The resistive heater is powered at 5 W and is fired 1 s before initiating the current ramp. As the heater remains powered throughout the ramp and quench processes, the net energy dissipation varies between ramp rates. This causes the conductor to quench at different points along the current excursion. An additional experiment is performed where the quench is initiated by a permanent magnet mounted directly to the CORC® conductor. In this configuration, the quench is initiated by a normal zone transition at a reduced critical current, which is relatively insensitive to current ramp rate. As a result, the experiment probes terminal current redistribution as a function of current ramp rate. A 3D printed permanent magnet fixture clamps directly to the CORC® wire and contains two samarium cobalt magnet cylinders (9.5 mm diameter x 10 mm height) generating approximately 0.4 Tesla on the conductor.

For both heater and permanent magnet induced quenches, baseline no-quench measurements are performed to measure the Hall sensor, sample voltage and current shunt

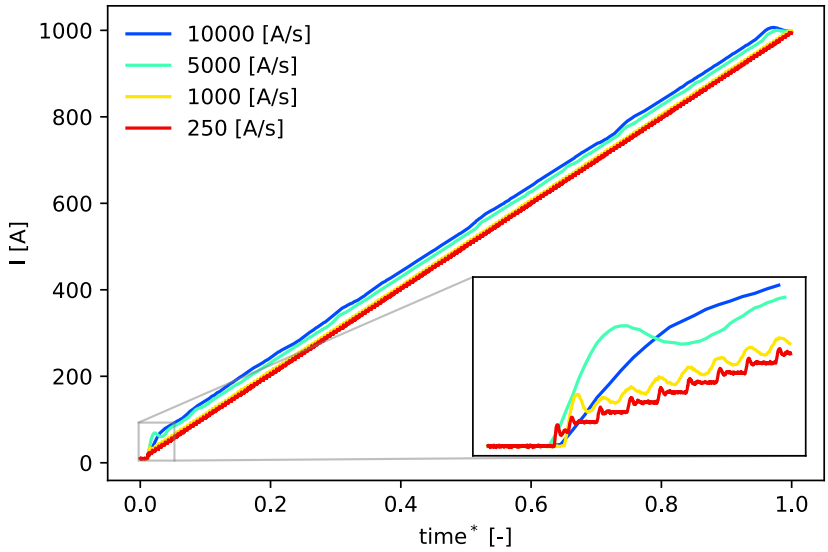

Figure 4. Power supply ramp profiles of shunt resistor current vs. non-dimensional time used on CORC® conductor.

voltages as a function of current ramp rate. These benchmark measurements are performed on the same day and thermal cycle as the quench tests. Results are then presented as the change in Hall sensor response between the baseline and quenched ramp tests.

2.3. Experimental

The CORC® wire provided by ACT consists of 8 layers with 2 tapes per layer and an average tape twist pitch of 5.6 mm. Tapes are oriented with the superconducting layer in compression, and each ReBCO layer is terminated approximately 20 mm apart over the 150 mm terminal. The SuperPower tapes are 2 mm wide with a 30 μm substrate, and have an average critical current of 78 A at 77 K. The as-manufactured CORC® sample has a critical current and n-value of 1,275 A and 25.5, respectively, measured at 76 K (liquid nitrogen boiling point in Boulder, CO) with a 1 μV/cm criterion.

The bespoke PCB Hall array was previously developed to measure current redistribution and quench propagation velocity in CORC® wires [29]. The array consists of 29 AKM HG-106A GaAs Hall sensors with a sensor spacing of 2 mm, and is powered by a 5 V supply. The Hall arrays monitor a length of 58 mm, and thus variations in magnetic field caused by changes in the current of the outermost and innermost layers are not captured (see Fig. 2 and Fig. 3). The center of the quench heater and permanent magnet are located 125 mm and 150 mm from the inside edge of the CORC® termination, as shown in Fig. 3. The voltage over the CORC® wire is measured with voltage contacts located within the sample terminations. These taps measure both the resistive voltage associated with current injection into the superconducting tapes and the voltage associated with the superconducting-to-normal transition of the CORC® wire.

A 32 channel Yokogawa WE707273 digitizer measures the 29 Hall sensors, the current shunt resistor, heater voltage and sample voltage. The data acquisition contains 16 bits of resolution over a range of ± 100 mV. The static experiments are measured at a rate of 1 kHz with a 50 Hz hardware lowpass filter, and the dynamic experiments are measured at a rate of 5 kHz with a 5 kHz hardware lowpass filter. After inducing a quench, the sample voltage triggers a quench protection system.

3. Results

3.1. Static quench

The results of the static quench experiments are shown in Fig. 5 at a constant current of 400 A (top), 700 A (middle) and 1,000 A (bottom). The colored contours show the change in Hall sensor voltage, on a scale from -50 μV to +300 μV. Sensor 0 corresponds to the inner-most (CORC® side) Hall sensor, and Sensor 28 corresponds to the outer-most Hall sensor (see Fig. 2). The corresponding sample voltage is shown in white on the right y-axis. To facilitate comparison between different quench experiments, the three plots are synchronized with the white vertical line corresponding to a sample voltage of 1 mV. It should be emphasized that the contours are not synchronized with heater initiation; the heater is fired 1.89 s, 1.25 s and 0.80 s before the vertical 1 mV marker for the 400 A, 700 A and 1,000 A experiments, respectively.

Fig. 5 shows clear Hall sensor responses originating from the onset of a normal zone initiation. In the 400 A case, all sensors rise synchronously with a similar magnitude. The sensor rise is attributed to current redistributing from the outer layer at the CORC® side of the terminal towards inner layers at the opposite side of the terminal. This propagates current further along the terminal, increasing the magnetic field in the vicinity of the PCB array. The largest signal change comes from sensors 15-25, and the smallest signal change comes from sensors 0-5.

With quenches at a current of 700 A and 1,000 A, a decrease in Hall sensor voltage is observed locally near sensors 0-10 (CORC® side). This response location suggests an outer-layer normal zone transition. Focusing now on the 700 A case (middle of Fig. 5), a wave-like normal zone propagation is observed between times of 0.4 to 0.65 s. Due to the helical structure of CORC®, a single-tape quench would produce a sinus-like depression of magnetic field at the local conductor pitch period. This general behaviour is observed (-0.05 to -0.025 mV contours), however the normal zone transition initiates at the side of the terminal opposite where the cable enters (sensor 26 at 0.4 s) and propagates towards the CORC® side of the terminal with time (sensor 7 at 0.45 s and sensor 0 at 0.53 s).

The magnitude of the change in Hall probe voltage after the heater is triggered depends on the overall current in the CORC® wire. At low operating current (for instance 400 A), a relatively high level of current redistribution from the tapes in the outer layers into tapes of the inner layers occurs after the heater causes the outer tape layers to transition. On the

other hand, current redistribution is more limited when the operating current of the CORC® wire is close to its critical current, because the tapes in the inner layers already carry close to the maximum current before the heater is triggered.

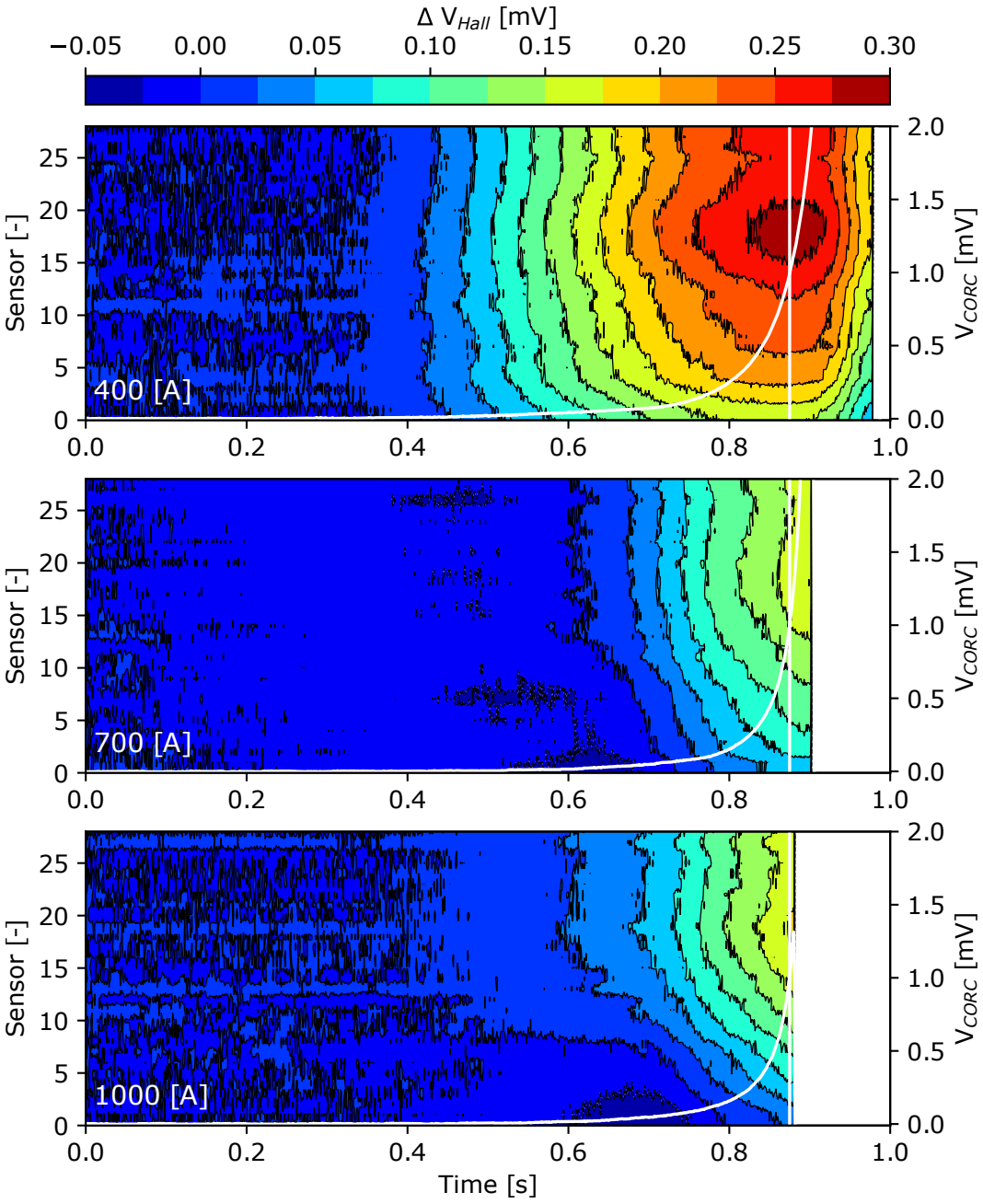

Figure 5. Hall sensor responses from static quench ($\Delta V_{Hall} = V_{quench} - V_{ref}$). Heater fired at 400 A (top), 700 A (middle) and 1,000 A (bottom). Sample voltage, shown in white, is displayed on right y-axis.

3.2. Dynamic quench

Fig. 6 shows the Hall sensor responses from a magnet-induced quench at 1,000 A/s (top), 5,000 A/s (middle) and 10,000 A/s (bottom). Contours are now presented as a function of current and range from -750 μV to +1000 μV. The sample voltage (white, right y-axis) exhibits an inductive voltage ripple following the power supply measurements in Fig. 4. The 5,000 and 10,000 A/s ramp rates show similar global behaviours as the static quench experiments, however with larger signal magnitudes and smaller responses in the vicinity of sensors 24-28. In contrast, the slower ramp case of 1,000 A/s shows the opposite behaviour, where all Hall sensor voltages decrease. This decreased Hall sensor response suggests current redistribution from inner CORC® layers to outer layers (Fig. 2). These experiments were repeated and the same behaviour was observed.

Fig. 7 shows the Hall sensor responses from a heater-induced quench at 1,000 A/s (top), 5,000 A/s (middle) and 10,000 A/s (bottom). Contours are presented with the same color scales as Fig. 6. As with the static quenches, the general trend shows an increase in measured field at the PCB array, commensurate with current axially displacing along the terminal. All of the dynamic ramp experiments (Fig. 6, Fig. 7) exhibit magnetic features near sensors 7, 17 and 27. Small variations in Hall sensor sensitivity and dynamic response may be responsible for the horizontal bands at these sensor locations. Another possible explanation arises from the tape topology inside the CORC terminal.

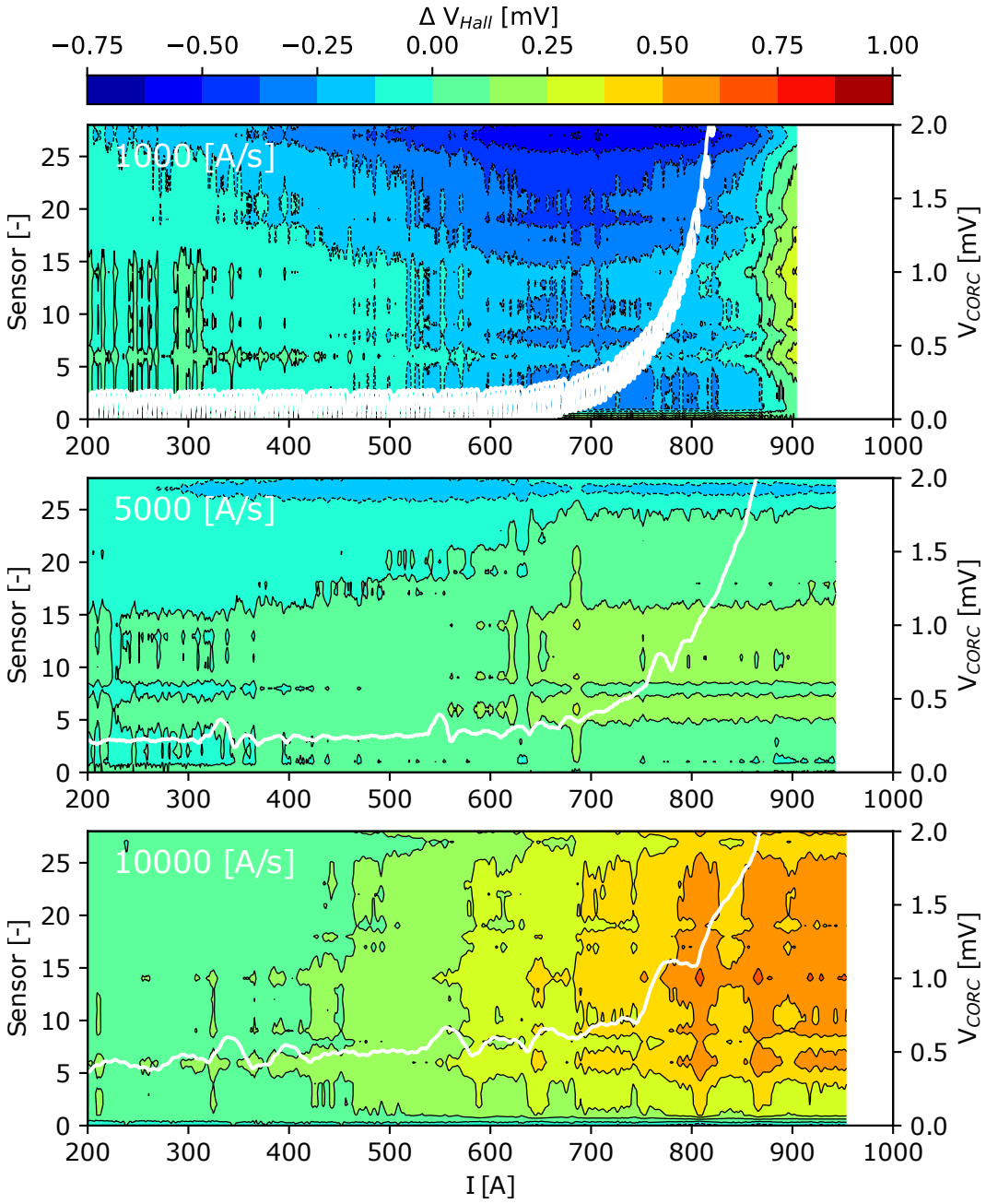

Figure 6. Dynamic quench results with permanent magnet induced quench. Current is ramped from 0 to 1,000 A at a rate of 1,000 A/s (top), 5,000 A/s (middle) and 10,000 A/s (bottom).

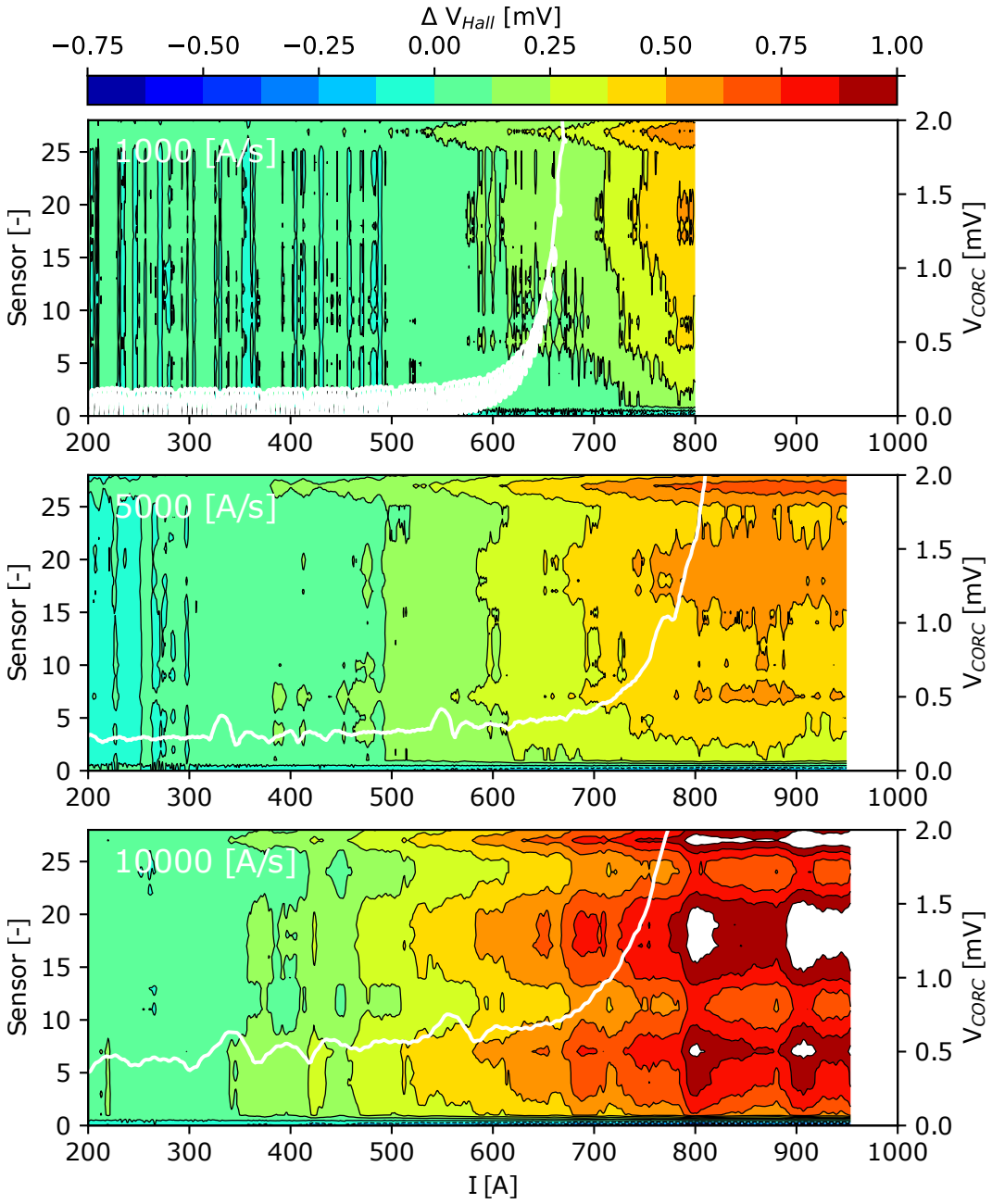

Figure 7. Dynamic quench results with heater induced quench. Current is ramped from 0 to 1,000 A at a rate of 1,000 A/s (top), 5,000 A/s (middle) and 10,000 A/s (bottom).

4. Discussion

The contour plots above show the change (ΔV_{Hall}) in Hall sensor voltages with a normal zone transition. In an effort to understand how current fills the conductor, Fig. 8 shows the raw terminal Hall sensor distribution (V_{Hall}) as a function of current for slow, near-static (top, 60 A/s) and dynamic (bottom, 10,000 A/s) ramps. Both contours show a positive ramp from 0 to 1,000 A with no quench. With a 60 A/s ramp rate, the measured magnetic field is nearly homogeneous at 100 Amps; the 5 mV contour line is almost vertical, suggesting a relatively uniform distribution of contact resistances. The magnitude of the Hall sensor responses gives insight into the small current perturbations induced by normal zone transitions. Consider the 400 A static quench experiment in Fig. 5; the 0.275 mV response of sensors 15-28 corresponds to a 5 A displacement in current along the terminal, assuming a line current as depicted in Fig. 2.

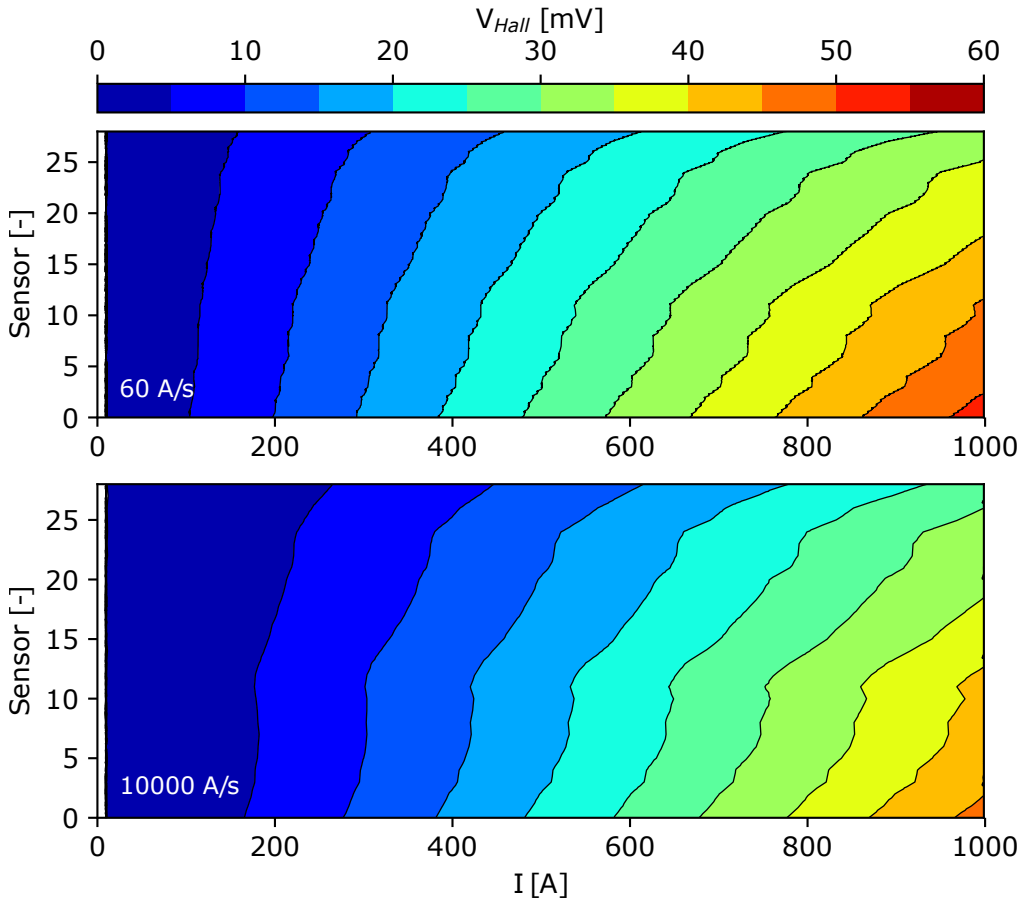

Figure 8. Evolution of Hall sensor voltage magnitudes as a function of space and current with 60 A/s (top) and 10,000 A/s (bottom).

Fig. 9 shows the difference between the slow (60 A/s) and fast-ramped (10,000 A/s) Hall sensor voltages of Fig. 8, revealing the terminal magnetic field evolution arising solely from inductive voltages. The fast-ramped Hall sensor voltages are homogeneously suppressed for

currents up to 200 A (vertical red-yellow contour lines), at which point spatial field variations begin to form. Differences between slow and fast-ramped distributions (i.e., the magnitude of the contours) diminish with currents beyond 850 A; analogous behaviour was observed in Ref. [28], where the largest hysteretic deviation in CORC® sample voltage was observed at intermediate current values in fast-ramped I-V characterizations.

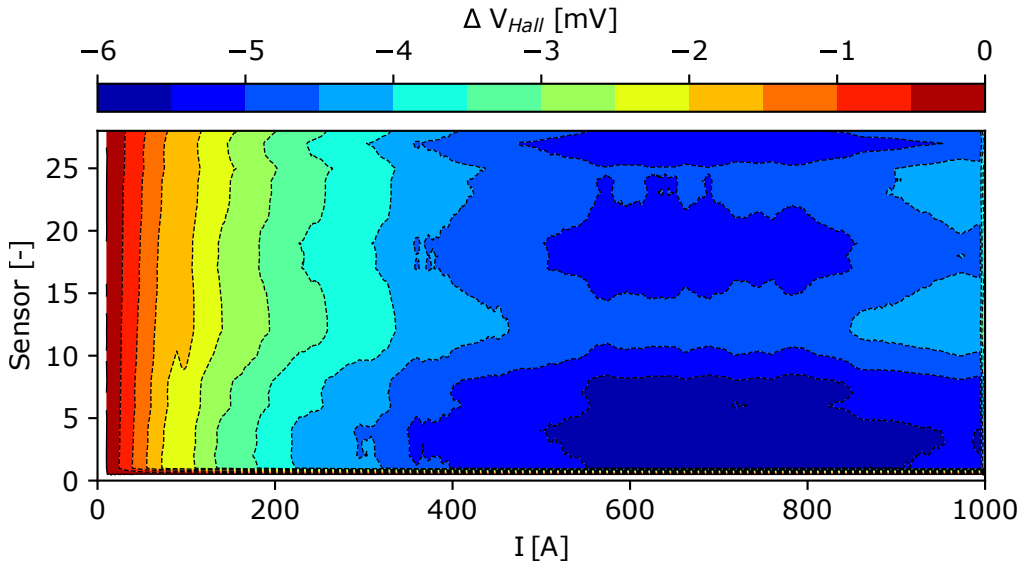

Figure 9. Change in Hall sensor voltages between the slow (60 A/s) and fast-ramped (10,000 A/s) experiments of Fig. 8, showing the difference in terminal field due to inductive voltages (i.e., no quench).

Fig. 10 shows the Hall sensor responses for both up (0-1,000 A) and down (1,000-0 A) ramps at rates of 1,000 A/s (top), 5,000 A/s (middle) and 10,000 A/s (bottom). The left column shows no-quench ramps (trapezoidal current profile with 0.2 s dwell) and the right column shows fast-ramped, permanent magnet-induced quench experiments. The non-negligible hysteresis loop is attributed mainly to tape inductances (see Fig. 9), however further work is required to quantify potential contributions from the dynamic Hall sensor response and shielding currents in the bulk terminal assembly. The large loop in the right column is caused by the rapid $-di/dt$ of the triggered quench detection system. Finally, it is important to reiterate that the contour plots of Fig. 6 and Fig. 7 show the difference between positive ramps in the left and right Hall array responses of Fig. 10.

Fig. 11 shows the static quench data (Fig. 5) in the context of a real-time quench detection system. The colored lines show the Hall sensor responses (blue, sensor 0) on the same scale as the sample voltage (black dotted line). In the 400 A case, the Hall sensor and sample voltages show signs of transition near 0.15 s, however the magnitude of the Hall sensor response exceeds that of traditional voltage measurements. In the 1,000 A case, the Hall sensor response precedes the rise of the sample voltage near 0.25 s.

The fast-ramped quench experiments are encouraging, although an implementation challenge is introduced for real-time quench detection. A quench detection system compares

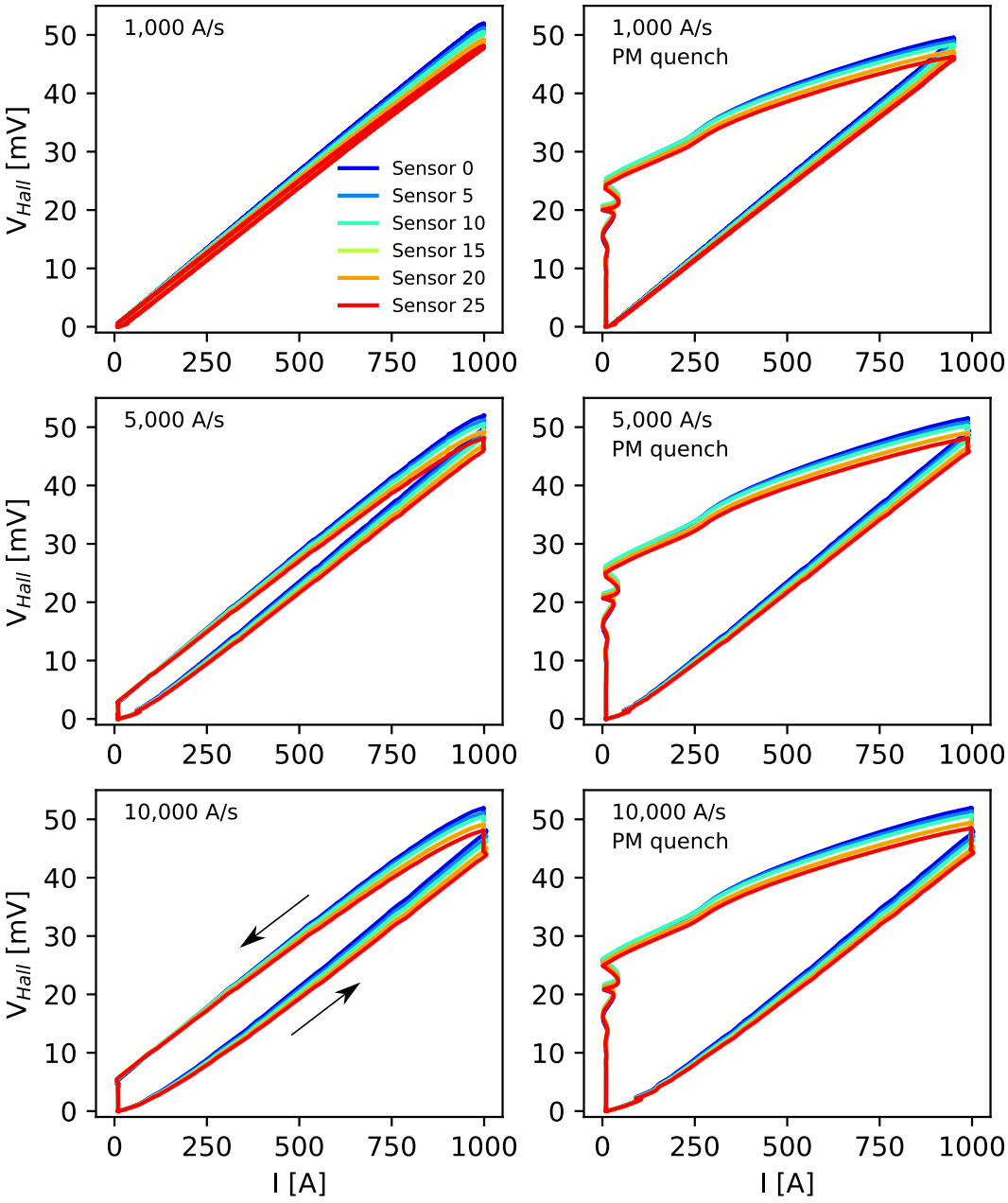

Figure 10. Measured Hall sensor hysteresis loop with ramp rates of 1,000 A/s (top), 5,000 A/s (middle) and 10,000 A/s (bottom). Left column shows no quench and right column shows permanent magnet induced quench.

expected and measured sensor values; if the difference exceeds a threshold, a quench trigger is generated. In the dynamic case, a set of training ramps would be required that may be unique to each installation. These data would be well-suited to fit the parameters of a phenomenological model or train a sequence classifier (i.e., recurrent neural network or support vector machine). This could theoretically provide years of magnet health monitoring (both quench detection and tape damage detection) in a Fusion device, although the method

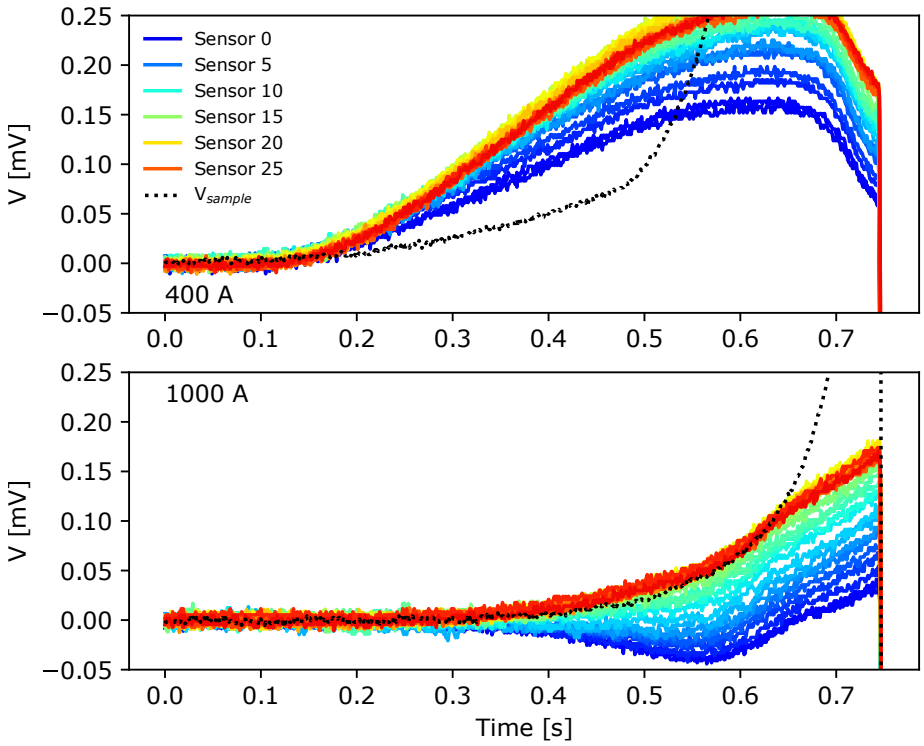

Figure 11. Comparison of Hall sensor voltages (colored from sensor 0, blue, to sensor 29, red) and sample voltage (black dotted line) in static quench at 400 A (top) and 1,000 A (bottom).

relies on alternative quench detection methods in the generation of training data.

To detect quenches using terminal magnetic field measurements, current sharing must be limited between tapes. Although this was shown to be a valid assumption for the 0.2 meter conductor, future work will explore Hall sensor quench detection in longer samples, with varied inter-tape contact resistances and at 4.2 K to identify the limitations of the technique. A particularly promising application for the methodology is the six-around-one CORC® Cable-In-Conduit Conductor (CICC) [30], as current is not shared significantly between separate CORC® cables. This is analogous to the methodology originally developed by Marchevsky *et al* (2010) [19], and the results here (i.e., Fig. 11) suggest that the terminal Hall array could be highly effective in monitoring quenches in CORC® CICC.

5. Conclusion

An experimental campaign is performed to assess the quench-detection capabilities of CORC® cable terminations with embedded Hall sensors. Static and fast-ramped quench experiments reveal a repeatable and measurable current redistribution in the terminal. In the static case, it is found that the Hall sensors detect normal zone transitions with a similar magnitude and temporal resolution as voltage measurements. Similar success is achieved in fast-ramp quench experiments, however adoption as a real-time quench detection technique relies on training datasets to fit the response of the nonlinear and hysteretic Hall sensors. Although the presented results demonstrate the value of this methodology as both a quench detection method and as an instrument to probe current dynamics in CORC® cables, additional experiments with longer samples are required to explore the limitations of the technique.

Acknowledgments

This work was supported by the Director, Office of Science, High Energy Physics, U.S. Department of Energy under contract No. DE-AC02-05CH11231, DE-SC0014009 and DE-SC0019934.

References

[1] A. Xu, Y. Zhang, M. H. Gharahcheshmeh, Y. Yao, E. Galstyan, D. Abraimov, F. Kametani, A. Polyanskii, J. Jaroszynski, V. Griffin, G. Majkic, D. C. Larbalestier, and V. Selvamanickam. J e (4.2 K, 31.2 T) beyond 1 kA/mm2 of a ˜3.2 m thick, 20 mol% Zr-added MOCVD REBCO coated conductor. *Scientific Reports*, 7(1):6853, December 2017.

[2] J. van Nugteren, G. Kirby, J. Murtomaki, G. DeRijk, L. Rossi, and A. Stenvall. Toward REBCO 20 T+ Dipoles for Accelerators. *IEEE Transactions on Applied Superconductivity*, 28(4):4008509, June 2018.

[3] X. Wang, S. A. Gourlay, and S. O. Prestemon. Dipole Magnets Above 20 Tesla: Research Needs for a Path via High-Temperature Superconducting REBCO Conductors. *Instruments*, 3(4):62, November 2019.

[4] D. Uglietti. A review of commercial high temperature superconducting materials for large magnets: from wires and tapes to cables and conductors. *Superconductor Science and Technology*, 32(5):053001, May 2019.

[5] P. Bruzzone, W. H. Fietz, J. V. Minervini, M. Novikov, N. Yanagi, Y. Zhai, and J. Zheng. High temperature superconductors for fusion magnets. *Nuclear Fusion*, 58(10):103001, October 2018.

[6] D. G. Whyte, J. Minervini, B. LaBombard, E. Marmar, L. Bromberg, and M. Greenwald. Smaller & Sooner: Exploiting High Magnetic Fields from New Superconductors for a More Attractive Fusion Energy Development Path. *Journal of Fusion Energy*, 35(1):41–53, February 2016.

[7] B.N. Sorbom, J. Ball, T.R. Palmer, F.J. Mangiarotti, J.M. Sierchio, P. Bonoli, C. Kasten, D.A. Sutherland, H.S. Barnard, C.B. Haakonsen, J. Goh, C. Sung, and D.G. Whyte. ARC: A compact, high-field, fusion nuclear science facility and demonstration power plant with demountable magnets. *Fusion Engineering and Design*, 100:378–405, November 2015.

[8] F. Scurti, S. Ishmael, G. Flanagan, and J. Schwartz. Quench detection for high temperature

superconductor magnets: a novel technique based on Rayleigh-backscattering interrogated optical fibers. *Superconductor Science and Technology*, 29(3):03LT01, March 2016.

[9] D. van der Laan, J. Weiss, S. Federico, and J. Schwartz. CORC® wires with integrated optical fibers for temperature and strain monitoring and voltage wires for reliable quench detection. *Submitted to Superconductor Science and Technology*, 2020.

[10] Y. Iwasa. Mechanical disturbances in superconducting magnets - a review. *IEEE Transactions on Magnetics*, 28(1):113–120, January 1992.

[11] M. Marchevsky, G. Ambrosio, M. Lamm, M. A. Tartaglia, and M. L. Lopes. Localization of Quenches and Mechanical Disturbances in the Mu2e Transport Solenoid Prototype Using Acoustic Emission Technique. *IEEE Transactions on Applied Superconductivity*, 26(4):4102105, June 2016.

[12] E. Ravaioli, M. Martchevskii, G. Sabbi, T. Shen, and K. Zhang. Quench Detection Utilizing Stray Capacitances. *IEEE Transactions on Applied Superconductivity*, 28(4):4702805, June 2018.

[13] A. Ninomiya, K. Sakaniwa, H. Kado, T. Ishigohka, and Y. Higo. Quench detection of superconducting magnets using ultrasonic wave. *IEEE Transactions on Magnetics*, 25(2):1520–1523, March 1989.

[14] T. Ishigohka, O. Tsukamoto, and Y. Iwasa. Method to detect a temperature rise in superconducting coils with piezoelectric sensors. *Applied Physics Letters*, 43(3):317–318, August 1983.

[15] M. Marchevsky, E. Hershkovitz, X. Wang, S. A. Gourlay, and S. Prestemon. Quench Detection for High-Temperature Superconductor Conductors Using Acoustic Thermometry. *IEEE Transactions on Applied Superconductivity*, 28(4):4703105, June 2018.

[16] D. Leroy, J. Krzywinski, V. Remondino, L. Walckiers, and R. Wolf. Quench observation in LHC superconducting one meter long dipole models by field perturbation measurements. *IEEE Transactions on Applied Superconductivity*, 3(1):781–784, March 1993.

[17] T. Ogitsu, A. Devred, K. Kim, J. Krzywinski, P. Radusewicz, R.I. Schermer, T. Kobayashi, K. Tsuchiya, J. Muratore, and P. Wanderer. Quench antenna for superconducting particle accelerator magnets. *IEEE Transactions on Magnetics*, 30(4):2273–2276, July 1994.

[18] M. Marchevsky, G. Sabbi, S. Prestemon, T. Strauss, S. Stoynev, and G. Chlachidze. Magnetic Quench Antenna for MQXF Quadrupoles. *IEEE Transactions on Applied Superconductivity*, 27(4):9000505, June 2017.

[19] M. Marchevsky, Y-Y Xie, and V. Selvamanickam. Quench detection method for 2G HTS wire. *Superconductor Science and Technology*, 23(3):034016, March 2010.

[20] T. Kato, H. Tsuji, T. Ando, Y. Takahashi, H. Nakajima, M. Sugimoto, T. Isono, N. Koizumi, K. Kawano, M. Oshikiri, and others. First test results for the ITER central solenoid model coil. *Fusion Engineering and design*, 56:59–70, 2001.

[21] D. C. van der Laan. YBa $_2$ Cu $_3$ O $_7$ coated conductor cabling for low ac-loss and high-field magnet applications. *Superconductor Science and Technology*, 22(6):065013, June 2009.

[22] D. C. van der Laan, P. D. Noyes, G. E. Miller, H. W. Weijers, and G. P. Willering. Characterization of a high-temperature superconducting conductor on round core cables in magnetic fields up to 20 T. *Superconductor Science and Technology*, 26(4):045005, April 2013.

[23] D. C. van der Laan, J. D. Weiss, and D. M. McRae. Status of CORC ® cables and wires for use in high-field magnets and power systems a decade after their introduction. *Superconductor Science and Technology*, 32(3):033001, March 2019.

[24] J. D. Weiss, D. C. van der Laan, D. Hazelton, A. Knoll, G. Carota, D. Abraimov, A. Francis, M. A. Small, G. Bradford, and J. Jaroszynski. Introduction of the next generation of CORC ® wires with engineering current density exceeding 650 A mm ^{2} at 12 T based on SuperPower's ReBCO tapes containing substrates of 25 m thickness. *Superconductor Science and Technology*, 33(4):044001, April 2020.

[25] D. van der Laan. Superconducting cable connections and methods, September 2017. US patent 9,755,329.

[26] D. van der Laan. Superconducting cable connections and methods, June 2019. European Patent 3008777.

[27] Fabrizio Bellina and Marco Ghin. Analysis of the Prototype Joints between Superconducting Cables of ITER CS Coils. *Fusion Technology*, 34(3P2):669–674, 1998.

[28] P. C. Michael, L. Bromberg, D. C. van der Laan, P Noyes, and H W Weijers. Behavior of a high-temperature superconducting conductor on a round core cable at current ramp rates as high as 67.8 kA/s in background fields of up to 19 T. *Superconductor Science and Technology*, 29(4):045003, April 2016.

[29] M. Marchevsky, E. Hershkovitz, S. Prestemon, J. Weiss, and D. van der Laan. Acoustic and magnetic detection of hot spots in superconducting CORC® cables. ASC 2018, 1LOr2C-06.

[30] T. Mulder, A. Dudarev, M. Mentink, M. Dhalle, and H. Ten Kate. Development of Joint Terminals for a New Six-Around-One ReBCO-CORC Cable-in-Conduit Conductor Rated 45 kA at 10T/4K. *IEEE Transactions on Applied Superconductivity*, 26(3):4801704, 2016.